Diffraction radiation from an ultrarelativistic charge in the plasma frequency limit

A. A. Tishchenko,[1,*] A. P. Potylitsyn,[2] and M. N. Strikhanov[1]
[1]*Moscow Engineering Physics Institute (State University), Kashirskoe sh. 31,115409 Moscow, Russia*
[2]*Tomsk Polytechnic University, Pr. Lenina 2a, 634050 Tomsk, Russia*
(Received 16 February 2004; revised manuscript received 29 June 2004; published 20 December 2004)

Diffraction radiation (DR) from an ultrarelativistic particle in the high frequency limit is considered. The distribution of the emitted energy over angles and frequencies has been obtained. Both backward DR and forward DR have been explored. The maximum of backward DR is found to augment with increasing the oblique incidence angle.

DOI: 10.1103/PhysRevE.70.066501 PACS number(s): 41.60.−m, 52.59.−f

I. INTRODUCTION

Diffraction radiation (DR) arises when a charged particle moves near the edge of a target [1–6]. By now the model of the perfect conducting target has been explored in detail. Thus in Ref. [7] DR from a charge passing near an infinitely thin perfectly conducting semi-infinite plane has been calculated exactly. A similar problem has been investigated in Ref. [8] for a metal wedge with arbitrary vertex angle. Results of the studies [1–8] relating to DR are restricted to optical frequencies.

On the other hand, transition radiation (TR) of an ultrarelativistic charge extends to the region of high frequencies up to $\gamma\omega_p$ [6]. Here γ is the Lorenz factor of the charge, $\omega_p=\sqrt{4\pi ZNe^2/m}$ is the plasma frequency, N is the number density of atoms, m is the mass of the electron, Z is the number of the atomic element in the periodic table. With that TR is a constant at frequencies from ω_p to $\gamma\omega_p$, and decreases as ω^{-4} at frequencies $\omega>\gamma\omega_p$. TR and DR have the same nature—they arise owing to dynamic polarization of the material by the proper field of the passing charge. This allows us to assume a similar behavior for DR.

DR in the plasma frequency limit ($\omega\gg\omega_p$) has been already investigated. DR for the nonrelativistic case $\beta\ll 1$ was considered in Ref. [9]. However, DR is well known to be nonzero only if the distance between the target and the charge is not larger than $\beta\gamma\lambda$. Hence there is not any reason to consider DR in the high frequency limit for nonrelativistic particles. Theoretical description of the x-ray generation through resonant DR (the Smith-Purcell effect) is given in Ref. [10]. This approach is based on the equations given in Ref. [4] (p. 382), which had been obtained for an infinitely thin perfectly conducting target. This makes the applicability of these results for frequencies larger than optical ones rather questionable. Moreover, the skin effect does not occur at frequencies $\omega>\omega_p$ and the approximation of infinitely thin target is not valid.

The study of DR at high frequencies has a practical importance for the development of novel methods of noninterceptive diagnostics of charged particle beams. Therefore it is of interest to explore the DR of an ultrarelativistic charge at frequencies larger than ω_p in detail.

In the present paper we use a simple method, which allows us to obtain the main characteristics of DR. This method was suggested by Durand [11] and applied for the exploring of TR at frequencies $\omega\gg\omega_p$.

Our approach is based on the fact that media become transparent for the radiation at frequencies of interest. Due to this fact one can neglect reflection and refraction of the radiation on the surface of the target. The virtue of this approach follows from its simplicity and applicability to different geometries of the problem. Here we have considered a case when an ultrarelativistic charge moves uniformly above the slab parallel to its top plane. The oblique incidence angle, the width, and thickness of the slab are supposed to be arbitrary. In Sec. II and III we derive the expression for the current density induced in the slab and give the general expression for the distribution of the emitted energy over angles and frequencies. In Sec. IV we consider a special case when the charge trajectory is crossed with the plane of the slab under right angle. The case of arbitrary oblique incidence angle is discussed in Sec. V. In Sec. VI we summarize the main features of DR at high frequencies and discuss the scope of validity of the results.

II. CURRENT DENSITY INDUCED IN THE SLAB

Let us consider DR from an ultrarelativistic charge passing close to a single target. We will take the slab with sizes $a\times\infty\times b$ as a target (see Fig. 1). In reality, the slab length can be considered as infinite, if it is more than $\gamma\lambda$.

Assume that the charge travels at constant velocity $\mathbf{v}=(v_x,v_y,0)$. At the moment $t=0$ it is at the point $(0,0,h)$. The proper field of the charge induces a current in the slab substance. The radiation arising here is defined by the Fourier image of the current density $\mathbf{j}(\mathbf{p},\omega)$. The connection of the polarization current density $\mathbf{j}(\mathbf{r},\omega)$ with the proper charge field $\mathbf{E}_0$ can be written as

$$\mathbf{j}(\mathbf{r},\omega)=\frac{\omega}{4\pi i}[\varepsilon(\omega)-1]\mathbf{E}_0(\mathbf{r},\omega). \tag{1}$$

At high frequencies

*Corresponding author. Fax: (095) 324-0425. Email address: tishchenko@dpt39.mephi.ru

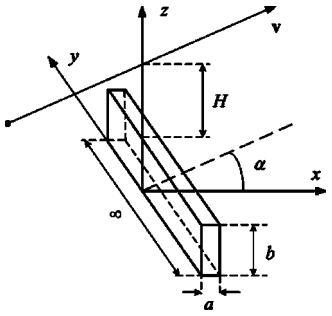

FIG. 1. The geometry. H is an impact parameter, b is the width of the slab, a is the thickness, α is the oblique incidence angle, i.e., the angle between the velocity $\mathbf{v}$ and axis x. The charge moves parallel to the xy plane.

$$\omega \gg \omega_p \tag{2}$$

a dielectric function has a universal form [12]

$$\varepsilon = 1 - \omega_p^2/\omega^2. \tag{3}$$

Consider a high energetic particle with

$$\gamma \gg 1. \tag{4}$$

In this case the charge field $\mathbf{E}_0$ is nearly transverse with respect to $\mathbf{v}$ [4] and we can ignore the parallel component of it. The Fourier image of the transverse proper field $\mathbf{E}_\perp$ of the ultrarelativistic charged particle is

$$\mathbf{E}_\perp(\mathbf{q},\omega) = -\frac{ie}{2\pi^2}\frac{\mathbf{q} - \mathbf{v}\omega/v^2}{q^2 - \omega^2/c^2}\delta(\omega - \mathbf{q}\cdot\mathbf{v})\exp\{-iq_z h\}. \tag{5}$$

Thus within the range of inequalities (2) and (4) the polarization current density becomes

$$\mathbf{j}(\mathbf{r},\omega) = \frac{i\omega}{4\pi}\frac{\omega_p^2}{\omega^2}\int d^3q \mathbf{E}_\perp(\mathbf{q},\omega)\exp\{i\mathbf{q}\cdot\mathbf{r}\}. \tag{6}$$

III. RADIATION FIELD AND EMITTED ENERGY

At frequencies $\omega \gg \omega_p$ the refraction coefficient differs from unity only in the quantity of the order of $(\omega_p/\omega)^2$. On the other hand, the polarization current density is proportional to $(\omega_p/\omega)^2$. Consequently, taking into account refraction and reflection gives terms of the order of $(\omega_p/\omega)^4$ that can be neglected. Hence we can ignore reflection and refraction on the slab surface at frequencies of interest. Therefore the radiation formed inside the slab goes out without changes both in amplitude and direction. In other words, we assume here rectilinear propagation of the radiation from the source point to the surface of the slab with a real wave vector $\sqrt{\varepsilon}\mathbf{k}$ and rectilinear propagation to the point of observation with a wave vector $\mathbf{k}$. This approach has been applied successfully by Durand [11] for analysis of TR at high frequencies (see also Ref. [6]). Besides, a similar method was used within the frame of eikonal approximation [13]. The radiation field here can be obtained as

$$\mathbf{E}^r(\mathbf{r},\omega) = \frac{\exp\{ikr\}}{r}\frac{i\omega}{c^2}\mathbf{n}\times\mathbf{n}\times\int_V d^3r' \times\exp\{-i\sqrt{\varepsilon}\mathbf{k}\cdot\mathbf{r}'\}\mathbf{j}(\mathbf{r}',\omega), \tag{7}$$

where $\mathbf{k} = (\omega/c)\mathbf{n}$ is the wave vector of the radiation field at the point of observation, $\mathbf{n}$ is the unit vector. We are integrating here over all volume V of the slab. The result of integrating is

$$\mathbf{E}^r(\mathbf{r},\omega) = \frac{\exp\{ikr\}}{r}\frac{e\omega_p^2}{c^2}\frac{1-\exp\{ia\varphi\}}{4\pi v_x\varphi}\exp\{-H\rho\} \times\frac{\exp\{-ibk_z\} - \exp\{-b\rho\}}{\rho - i\sqrt{\varepsilon}k_z}\mathbf{n}\times\mathbf{n}\times\left(\frac{\mathbf{A}}{\rho} - i\mathbf{e}_z\right). \tag{8}$$

Here is denoted

$$\varphi = \frac{k}{\beta_x}(1 - \mathbf{n}\cdot\mathbf{v}\sqrt{\varepsilon}/c), \quad v_x \neq 0, \quad \sqrt{\varepsilon} \simeq 1 - \frac{1}{2}\frac{\omega_p^2}{\omega^2}, \tag{9}$$

$$\rho = \frac{\omega}{c\beta_x\gamma}\sqrt{1 + \gamma^2(\varepsilon\beta^2 n_y^2 + \beta_y^2 - 2\sqrt{\varepsilon}\beta_y n_y)}, \tag{10}$$

$$\mathbf{A} = \left\{\frac{\omega}{v_x}\left(\frac{v_y^2}{v^2} - \sqrt{\varepsilon}\beta_y n_y\right), -\frac{\omega}{v}\left(\frac{v_y}{v} - \sqrt{\varepsilon}\beta n_y\right), 0\right\}. \tag{11}$$

Here H is the impact parameter, i.e., the shortest distance between the particle trajectory and the edge of the slab; a and b are the thickness and the width of the slab, respectively (see Fig. 1).

The spectral and angular distribution of the radiated energy can be found by the formula

$$d^2E(\mathbf{n},\omega) = cr^2 d\Omega d\omega|\mathbf{E}^r(\mathbf{r},\omega)|^2. \tag{12}$$

If we substitute Eq. (8) in Eq. (12), we get

$$\frac{d^2E(\mathbf{n},\omega)}{d\Omega d(\hbar\omega)} = \frac{e^2}{c\hbar}\left(\frac{\omega_p^2}{2\pi\omega^2}\right)^2 F_b\frac{1 - n_z^2 + [A^2 - (\mathbf{A}\cdot\mathbf{n})^2]/\rho^2}{(c^2/\omega^2)\rho^2 + \varepsilon n_z^2} \times\exp\{-2H\rho\}\frac{\sin^2\left(\frac{a\omega}{2v_x}(1 - \mathbf{n}\cdot\mathbf{v}\sqrt{\varepsilon}/c)\right)}{(1 - \mathbf{n}\cdot\mathbf{v}\sqrt{\varepsilon}/c)^2}, \tag{13}$$

$$F_b(b,\omega) = 1 - 2\exp\{-b\rho\}\cos(b\sqrt{\varepsilon}k_z) + \exp\{-2b\rho\}. \tag{14}$$

The factor F_b defines the dependence of the radiated energy on the slab width. It should be noticed that Eq. (13) describes DR at distances much larger than the dimension of the emitting source. Furthermore, formulas (8)–(14) are given as they are obtained from Eq. (7). In further analysis one should neglect terms of the order of $(\omega_p/\omega)^2$ in comparison with unity according to Eq. (2).

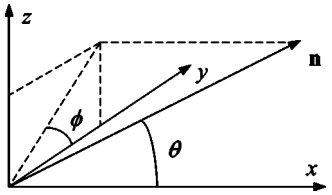

FIG. 2. Angles of observation.

IV. NORMAL INCIDENCE

Now we will consider the case when the velocity is directed along the x axis, i.e., $\alpha=0$, $\mathbf{v}=(v,0,0)$. It is easy to obtain

$$\frac{d^2E(\mathbf{n},\omega)}{d\Omega d(\hbar\omega)}=\frac{e^2}{c\hbar}\left(\frac{\omega_p^2}{2\pi\omega^2}\right)^2\frac{\sin^2\left(\frac{a\omega}{2v}(1-\sqrt{\varepsilon}\beta n_x)\right)}{(1-\sqrt{\varepsilon}\beta n_x)^2}\times F_b\frac{1-n_z^2+n_y^2(1-n_y^2)/(\gamma^{-2}+n_y^2)}{\gamma^{-2}+1-n_x^2}\exp\{-2H\rho\}, \tag{15}$$

where ρ becomes

$$\rho=\frac{\omega}{c\gamma}\sqrt{1+\gamma^2n_y^2} \tag{16}$$

and we have neglected terms of the order of γ^{-2} and ω_p^2/ω^2 in comparison with unity.

It is convenient to introduce the spherical coordinate system (see Fig. 2) as

$$n_x=\cos\theta,\quad n_y=\sin\theta\cos\phi,\quad n_z=\sin\theta\sin\phi. \tag{17}$$

We can see that the radiation has a sharp maximum for $\theta\sim\gamma^{-1}$. We have for $\theta\ll 1$

$$\frac{d^2E(\mathbf{n},\omega)}{d\Omega d\omega}\simeq\frac{1}{\pi^2}\frac{e^2}{c}\left(\frac{\omega_p}{\omega}\right)^4\frac{\sin^2\left[\frac{a\omega}{4c}(\theta^2+\gamma^{-2}+\omega_p^2/\omega^2)\right]}{(\theta^2+\gamma^{-2}+\omega_p^2/\omega^2)^2(\theta^2+\gamma^{-2})}\times F_b\frac{1+2\gamma^2n_y^2}{1+\gamma^2n_y^2}\exp\left\{-\frac{2H\omega}{c\gamma}\sqrt{1+\gamma^2n_y^2}\right\}. \tag{18}$$

Here $n_y\approx\theta\cos\phi$. It follows from Eq. (18) that maximal radiation is directed straightforward. The reason for it is the absence of any symmetry in reference to the charge trajectory.

A. Cutoff frequency

Let us look at the distinctive features of Eq. (18). First, there is a cutoff frequency ω_c. If

$$H<\lambda_p, \tag{19}$$

the cutoff frequency is

$$\omega_c\simeq\gamma\omega_p. \tag{20}$$

This is the same cutoff frequency as for TR. The condition (19) is rather exotic. It means that the trajectory of the particle almost touches the slab surface. In the case of

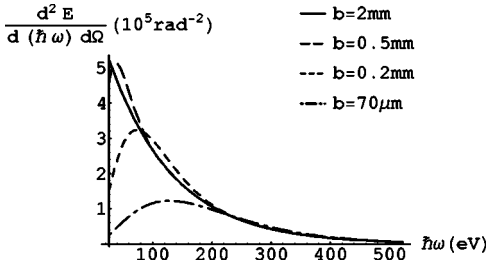

FIG. 3. DR emitted in the case $\alpha=0$ at $\theta=\gamma^{-1}$, $n_y=0$ for different values of the slab width b. The plasma frequency is $\omega_p=4.1\times10^{16}$ s^{-1}, $\hbar\omega_p=26.1$ eV (Beryllium). The impact parameter is $H=50$ μm; $\gamma=6\times10^4$. The thickness a may be any provided that Eq. (23) is fulfilled. For these parameters the cutoff frequency is $\hbar\omega_c=219$ eV. The figure is pictured using Eq. (13) within the frequency range from ω_p to 20 ω_p.

$$H>\lambda_p \tag{21}$$

the cutoff frequency is defined by the decreasing exponent and equals

$$\omega_c\simeq c\gamma/H. \tag{22}$$

The condition $H\gg\lambda_p$ is a practical case in experiments. In what follows we will assume Eq. (21) holds true and the cutoff frequency is $\omega_c\approx c\gamma/H$. In the considered case, this is much less than $\gamma\omega_p$. On account of this the sine in Eq. (18) oscillates rapidly with small changes in ω and can be replaced by its average value $1/2$ on condition

$$aH\pi^2\gg\lambda_p^2\gamma, \tag{23}$$

where $\lambda_p=2\pi c/\omega_p$. In this case Eq. (18) practically does not depend on ω_p and one can get the same formula as for optical diffraction radiation by a perfectly conducting, infinitely thin half plane, multiplied by 2 [5]:

$$\frac{d^2E(\mathbf{n},\omega)}{d\Omega d\omega}\simeq\frac{1}{2\pi^2}\frac{e^2}{c}\frac{\gamma^{-2}+2n_y^2}{(\theta^2+\gamma^{-2})(\gamma^{-2}+n_y^2)}\times\exp\left\{-2\frac{\omega}{\omega_c}\sqrt{1+\gamma^2n_y^2}\right\}. \tag{24}$$

In obtaining Eq. (24) for the sake of simplicity we have assumed $b=\infty$, i.e., $F_b=1$. Equation (24) differs from the analogous formula of Ref. [5] by multiplier 2. This multiplier corresponds to two independently emitting sides of the slab (at $x=0$ and $x=a$). The condition (23) is fulfilled, for instance, if $\omega_p=4\times10^{16}$ s^{-1} ($\hbar\omega_p=26.1$ eV, Beryllium [14]), $H\geqslant50$ μm, $a\geqslant10$ μm, $\gamma\leqslant10^5$. We will assume that Eq. (23) holds true in this section.

The cutoff frequency (22) depends on the Lorenz factor of the charge γ and the impact parameter H and does not depend on the properties of the material in contrast to the TR cutoff frequency $\gamma\omega_p$. The spectral density of the radiation spreads from ω_p up to $\omega_c\simeq c\gamma/H$ (see Fig. 3).

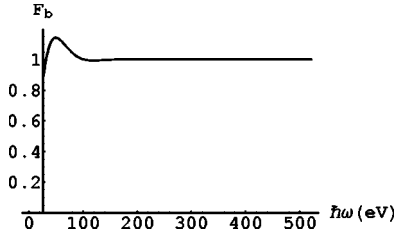

FIG. 4. The behavior of the factor $F_b(b,\omega)$. The parameters are the same as in Fig. 3, the thickness is $b=0.5$ mm. For these parameters the quantity $\omega_m \sim c\gamma/b$ equals 3.48×10^{16} s^{-1}. The figure is plotted using Eq. (13) within the frequency range from ω_p to $20\omega_p$.

B. Dependence on *b*

The energy emitted per frequency per solid angle depends on the width of the slab b by means of the factor $F_b(b,\omega)$ [see Eq. (14)]. For $b \gg \rho^{-1}$ ($\rho^{-1}=c\gamma/\omega$ at $n_y=0$) we have $F_b \approx 1$, i.e., any dependence of the radiation on the slab width b vanishes provided that b is large enough. For $b \ll \rho^{-1}$ we have $F_b \approx 2(1-\cos bk_z)$, i.e., oscillations of period λ/n_z appear, where λ is the wavelength. Thereby, the dependence of the radiated energy on the width of the slab b is defined by the ratio b to the effective width b_{eff},

$$b_{eff} \sim \rho^{-1} = \frac{c\gamma}{\omega\sqrt{1+\gamma^2 n_y^2}}. \tag{25}$$

In fact, b_{eff} is the characteristic distance for the decrease of the proper charge field. If the condition $n_y \leqslant \gamma^{-1}$ is satisfied we have $b_{eff} \sim \gamma\lambda$. For instance, for $n_y=0$, $\gamma \sim 6\times10^4$ and $\omega \sim 10^{17}$ s^{-1} we have $b_{eff} \approx 180$ μm.

Note that the maximum of the radiation falls at a frequency larger than ω_p and besides depends on the width b. This is because behavior of the function $F_b(b,\omega)$ is determined at fixed b by the ratio ω to some effective frequency of the order of

$$\omega_m \sim \gamma c/b. \tag{26}$$

Figure 4 demonstrates the behavior of the factor $F_b(b,\omega)$. All parameters are the same as in Fig. 3. Figure 3 shows the dependence of the radiated energy on the frequency at different values of the slab width b. If the width b increases further, the plot would not be changed significantly. Indeed, the dependence of the radiation on the width b vanishes at $b \gg b_{eff}$. Figure 3 shows a suppression of the radiation for $b \leqslant b_{eff}$ and $\omega \sim \omega_p$. Such a behavior is determined by the function $F_b(b,\omega)$; see Fig. 4.

C. Total radiated energy

Here we will consider the total energy radiated in the full solid angle at frequencies $\omega > \omega_p$. In order to make a rough estimation of the total radiated energy we should take the maximum of $d^2E(\mathbf{n},\omega)/d\Omega d\omega$ and multiply it by the width of the range where the radiation is maximal. As it follows from above, $(d\omega)_{eff} \sim \omega \sim \omega_c \sim c\gamma/H$, $(d\Omega)_{eff} \sim \gamma^{-2}$ provided that Eq. (21) holds true. Assuming that Eq. (23) is fulfilled, one obtains

$$E \sim \frac{1}{2\pi^2}\frac{e^2}{c}\frac{c\gamma}{H}\left[1-2\exp\left\{-\frac{b}{H}\right\}\cos\left(\frac{b}{H}\right)+\exp\left\{-\frac{2b}{H}\right\}\right]. \tag{27}$$

For $b \gg H$ we have

$$E \sim \frac{1}{2\pi^2}\frac{e^2}{c}\frac{c\gamma}{H}. \tag{28}$$

Thereby, the total radiated energy is proportional to the Lorenz factor γ. Note that such an estimation for TR gives $E \sim \frac{1}{3}(e^2/c)\gamma\omega_p$ which is greater than Eq. (28). This is connected mainly with the difference between the cutoff frequency for DR and TR: $c\gamma/H \ll \gamma\omega_p$. We emphasize that this estimation is rather rough and valid only for qualitative analysis.

V. OBLIQUE INCIDENCE

Now we go on to the discussion of the complete form of expression (13). First of all we will investigate the maxima of radiation. DR is a maximum when the index of the exponent $\exp\{-2H\rho\}$ is a minimum and the preexponential factor is maximal.

The inspection of ρ at fixed H, ω, and γ gives us the condition for which the exponent achieves its maximum,

$$n_y = \frac{\beta_y}{\beta^2\sqrt{\varepsilon}} = \frac{\sin\alpha}{\beta\sqrt{\varepsilon}}. \tag{29}$$

Here the angle α is defined by $\beta_x=\beta\cos\alpha$, $\beta_y=\beta\sin\alpha$ (see Fig. 1). With that, we have

$$\mathbf{A}=\mathbf{0},\ \rho=\frac{\omega}{c\gamma}. \tag{30}$$

Taking into account Eq. (29) we can see from Eq. (13) that the radiation is proportional to the factor

$$\frac{1-n_z^2+[A^2-(\mathbf{A}\cdot\mathbf{n})^2]/\rho^2}{(c^2/\omega^2)\rho^2+\varepsilon n_z^2} = \frac{1-n_z^2}{\gamma^{-2}+\varepsilon n_z^2}. \tag{31}$$

This factor is maximal if

$$n_z = 0. \tag{32}$$

This means that the radiation is maximal in the xy plane. Using Eqs. (32) and (29) one can see that there are two directions of maximal radiation. They are defined by

$$n_x = \pm\sqrt{1-\frac{\sin^2\alpha}{\beta^2\varepsilon}} = \pm\frac{\sqrt{\cos^2\alpha-(1-\varepsilon\beta^2)}}{\beta\sqrt{\varepsilon}}. \tag{33}$$

Here the sign "+" refers to the radiation maximum along the trajectory of the particle and the sign "−" refers to the radiation under the specular reflection angle. Hereafter we assume that

$$\omega \leqslant \omega_c = c\gamma/H \ll \gamma\omega_p. \tag{34}$$

The grazing incidence case, $\cos\alpha \leqslant \sqrt{1-\varepsilon\beta^2}$, requires a more detailed consideration and is not treated here. For $\cos\alpha$ large enough,

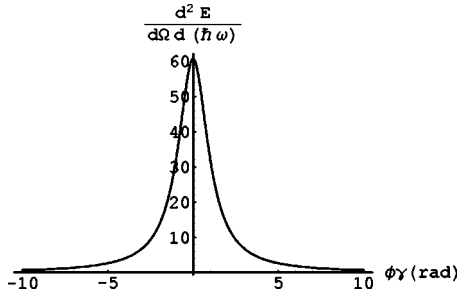

FIG. 5. The backward DR emitted at the angle $\theta=\pi-\alpha$, $\alpha=70°$. The frequency of observation is $\omega=10\omega_p$. The width of the slab is $b=0.5$ mm. The rest of the parameters are the same as in Fig. 3. The figure is plotted by Eq. (13) provided that Eq. (23) is satisfied.

$$\cos^2\alpha \gg 1-\varepsilon\beta^2 \approx \omega_p^2/\omega^2, \tag{35}$$

Eq. (33) takes on the form

$$n_x \approx \pm\frac{\cos\alpha}{\beta\sqrt{\varepsilon}}\left(1-\frac{\omega_p^2/\omega^2}{2\cos^2\alpha}\right). \tag{36}$$

Neglecting the second term in Eq. (36) one can see that there are two directions of the radiation in the *xy* plane:

$$\phi=0,\ \theta=\alpha,\quad \text{max FDR},$$

$$\phi=0,\ \theta=\pi-\alpha,\quad \text{max BDR}. \tag{37}$$

The former condition gives us the maximum of forward diffraction radiation (FDR). The latter condition means radiation emitted at the angle of specular reflection. This is called usually backward diffraction radiation (BDR). BDR is a rather convenient instrument for noninvasive diagnostics of charged particle beams [15] because the observation angle can be arbitrarily large. BDR in the optical range has been explored in detail by one of the authors of this study [16]. In particular, BDR was found to be emitted in the narrow cone like FDR (see Fig. 5).

Using Eqs. (29) and (36) one can get for FDR [sign "+" in Eq. (36)]

$$1-\mathbf{n}\cdot\mathbf{v}\frac{\sqrt{\varepsilon}}{c}\approx\frac{\omega_p^2}{2\omega^2} \tag{38}$$

and for BDR [sign "−" in Eq. (36)]

$$1-\mathbf{n}\cdot\mathbf{v}\frac{\sqrt{\varepsilon}}{c}\approx 2\cos^2\alpha. \tag{39}$$

The same expressions (38) and (39) can be obtained by using Eq. (37). The maximum of both FDR and BDR can be obtained from Eq. (13) allowing for Eqs. (30), (38), and (39). For the FDR maximum we have

$$\frac{d^2E_{\max}^{FDR}}{d\Omega d(\hbar\omega)}=\frac{e^2}{c\hbar}\frac{\gamma^2}{2\pi^2}\left[1-\exp\left\{-\frac{b\omega}{c\gamma}\right\}\right]^2\exp\left\{-\frac{2H\omega}{c\gamma}\right\}, \tag{40}$$

and for BDR we find

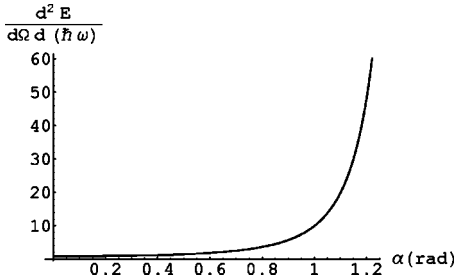

FIG. 6. The maximum of the backward DR emitted at angles $\phi=0$, $\phi=\pi-\alpha$, and frequencies $\omega=10\omega_p$, $\hbar\omega_p=26.1$ eV. The impact parameter is $H=50$ μm, $\gamma=6\times10^4$, $b=0.5$ mm. The thickness a may be any provided that Eq. (23) is satisfied. The figure is plotted by Eq. (41). The angle α changes from 0 to 70°.

$$\frac{d^2E_{\max}^{BDR}}{d\Omega d(\hbar\omega)}=\frac{e^2}{c\hbar}\frac{\gamma^2}{2\pi^2}\frac{(\omega_p/\omega)^4}{16\cos^4\alpha}\left[1-\exp\left\{-\frac{b\omega}{c\gamma}\right\}\right]^2\times\exp\left\{-\frac{2H\omega}{c\gamma}\right\}. \tag{41}$$

In obtaining Eqs. (40) and (41) and the sine square was replaced by $1/2$ according to the inequality (23). Comparing Eqs. (40) and (41) one can see that BDR is much weaker than FDR provided that Eq. (35) holds true. However, the BDR maximum increases with the angle α (see Fig. 6).

The factor

$$\left(\frac{\omega_p}{\omega}\right)^4\left[1-\exp\left\{-\frac{b\omega}{c\gamma}\right\}\right]^2$$

defines the law of BDR falling in the frequency range from ω_p to ω_c. The law of decreasing is ω^{-4} if

$$b\omega\gg c\gamma, \tag{42}$$

and it is ω^{-2} if

$$b\omega\ll c\gamma. \tag{43}$$

The condition (34) implies Eq. (43) if $b\ll H$. Practically, it can be a very thin lying slab ($a\gg b$) or a thin wire ($a\sim b$).

VI. SUMMARY

Now we go over the main points of our results. It is worth considering DR at $H>\lambda_p$ only in the frequency range

$$\omega_p<\omega<c\gamma/H. \tag{44}$$

At $\omega>c\gamma/H$ DR decreases as $\exp\{-\omega H/c\gamma\}$. In the opposite case $H<\lambda_p$ the trajectory of the charge almost touches the slab surface, DR becomes similar to TR, and the range where DR exists is

$$\omega_p<\omega<\gamma\omega_p. \tag{45}$$

The usual experimentation at $H\gg\lambda_p$, hence the cutoff frequency $\omega_c\simeq c\gamma/H$ depends only on the Lorentz factor γ and the impact parameter H. The spectral and angular density of the radiation has the maximum between ω_p and ω_c.

The slab width b plays a considerable part if $b\ll b_{eff}\sim\gamma\lambda$. In particular, decreasing b leads to radiation suppres-

sion at small frequencies, decreasing of the radiation maximum and shifting it towards high frequencies (see Fig. 3).

The essential distinction between DR and TR consists in their behavior at frequencies higher than the cutoff frequency: TR falls as ω^{-4} but DR falls as $\exp\{-\omega/\omega_c\}$. This exponential falling of DR can be used to determine the Lorenz factor of the charge. Namely, having measured ω_c and knowing the impact parameter H we can find $\gamma \sim H\omega_c/c$.

In practice the two-sided inequality (44) is satisfied if the charge has a very high energy so that $\gamma > 10^4$. To extend the range downwards one should use a material with the least plasma frequency. For example [14], the plasma frequency ω_p is 13.8 eV for lithium, 20.9 eV for polyethylene (CH_2), and 24.4 eV for mylar $(C_5H_4O_2)$.

For oblique incidence $\alpha \neq 0$ (see Fig. 1), the radiation maxima are defined by Eq. (29) $n_y = \beta_y/(\beta^2\sqrt{\varepsilon})$ as well as the condition $n_z = 0$. Equation (29) turns into the usual conditions for the FDR and BDR maxima (37), ignoring corrections of the order of γ^{-1}.

BDR is investigated. The BDR maximum is shown to augment with increasing angle α [see Eq. (41)]. It follows from above that BDR is rather weak in comparison with FDR. However, even relatively weak radiation can be of experimental interest since it is emitted at a large angle to the direction of motion. Furthermore, the smallness of the wavelength of the radiation gives a possibility to use such a radiation for submicron collider beams, where optical DR is unusable due to the diffraction limit.

The domain of validity of the main formula (13) is restricted to the inequalities $\omega > \omega_p$, $\gamma \gg 1$, and $\cos^2\alpha \gg \omega_p^2/\omega^2$. Besides, our results become nonapplicable at those frequencies where an imaginary part of the dielectric function in Eq. (3) should be taken into account. This might be narrow bands near the frequencies of characteristic absorption or frequencies higher or of the order of 1 MeV [17].

[1] B. M. Bolotovskii and G. V. Voskresenskii, Usp. Fiz. Nauk **94**, 377 (1968) [Sov. Phys. Usp. **11**, 143 (1968)].

[2] M. Castellano, Nucl. Instrum. Methods Phys. Res. A **394**, 275 (1997).

[3] R. B. Fiorito and D. W. Rule, Nucl. Instrum. Methods Phys. Res. B **173**, 67 (2001).

[4] M. L. Ter-Mikhaelyan, *High-Energy Electromagnetic Processes in Condensed Media* (Wiley, New York, 1972).

[5] A. P. Potylitsyn, Nucl. Instrum. Methods Phys. Res. B **145**, 169 (1998).

[6] P. Rullhusen, X. Artru, and P. Dhez, *Novel Radiation Sources Using Relativistic Electrons* (World Scientific, Singapore, 1998).

[7] A. P. Kazantsev and G. I. Surdutovich, Dokl. Akad. Nauk SSSR **147**, 74 (1962) [Sov. Phys. Dokl. **7**, 990 (1963)].

[8] A. I. Gilinskii, *Electromagnetic Surface Phenomena* (Nauka, Novosibirsk, 1990) (in Russian).

[9] J. C. McDaniel, D. B. Chang, J. E. Drummond, and W. W. Salisbury, Appl. Opt. **28**, 4924 (1989).

[10] M. J. Moran, Phys. Rev. Lett. **69**, 2523 (1992).

[11] L. Durand, Phys. Rev. D **11**, 89 (1975).

[12] L. D. Landau and E. M. Lifshitz, *The Electrodynamics of the Continuous Media* (Nauka, Moscow, 1992) (in Russian).

[13] A. I. Alikhanian and V. A. Chechin, Phys. Rev. D **19**, 1260 (1979).

[14] B. Dolgoshein, Nucl. Instrum. Methods Phys. Res. A **326**, 434 (1993).

[15] J. Urakawa *et al.*, Nucl. Instrum. Methods Phys. Res. A **472**, 309 (2001).

[16] A. P. Potylitsyn and N. A. Potylitsyna, Izv. Vyssh. Uchebn. Zaved. Fiz. **43**, 56 (2000) [Russ. Phys. J. **43**, 303 (2000)].

[17] G. M. Garibian and Y. Shi, *X-Ray Transition Radiation* (Publishing House of the Academy of Sciences of Armenian Republic, Yerevan, 1983) (in Russian).